

Correction of Cross-Peak Intensities in 2D Spin-Locked NOE Spectroscopy for Offset and Hartmann-Hahn Effects

AD BAX

*Laboratory of Chemical Physics, National Institute of Diabetes and Digestive and Kidney Diseases,
National Institutes of Health, Bethesda, Maryland 20892*

Received July 13, 1987; revised August 4, 1987

A method is described for semiquantitative evaluation of Hartmann-Hahn contributions to cross peaks in a spin-locked NOE (ROESY) experiment. Corrections are presented for the resonance offset effects on the resonance intensities and on NOE buildup rates. Relay of spin-locked NOE to other nuclei via the Hartmann-Hahn effect is treated in a similar fashion. Comparison of slices through the NOESY and ROESY spectra of a sample of BPTI is used to demonstrate the correction procedure. It is demonstrated that a recently proposed modification of the spin-locked NOE experiment, using small flip-angle pulses, does not offer any further suppression of Hartmann-Hahn contributions relative to the original experiment. © 1988 Academic Press, Inc.

The NOE effect is a powerful tool for determining molecular conformation in solution. For small molecules that have a correlation time (τ_c) that is fast relative to the reciprocal of the Larmor frequency (ω_L) the NOE is positive. For macromolecules ($\tau_c \gg 1/\omega_L$) the NOE is negative. Bothner-By and co-workers (1) have developed a spin-locked NOE method where the NOE is positive for all values of the correlation time, τ_c . This spin-locked NOE method is particularly useful for the study of intermediate size molecules (MW 800-2000) that typically exhibit very weak NOEs in the laboratory frame. The spin-locked NOE method can also be used for the study of macromolecules and offers a convenient method for distinguishing direct NOE effects from indirect (spin diffusion) effects (2).

The pulse scheme of the 2D spin-locked NOE experiment, often referred to as CAMELSPIN (1) or ROESY (3), is depicted in Fig. 1a. In this experiment a spin-lock field of constant phase is applied during the mixing period. The strength of the RF field is defined as ν . The effective field strength experienced by spin I in the rotating frame equals $\nu_I = \sqrt{(\delta_I^2 + \nu^2)}$, where δ_I is the offset of spin I from the carrier. Spurious cross peaks can occur in this type of NOE experiment if the effective field strengths, ν_I and ν_S , experienced respectively by two coupled spins I and S, are of nearly identical magnitude (3). For the case where $\nu_I = \nu_S$ (when spins I and S have identical but opposite offsets from the carrier) an oscillatory transfer of net magnetization takes place between the spin-locked components of the I and S spin magnetizations. A similar type of coherent magnetization transfer for detecting networks of scalar coupled spins has been described and exploited by Braunschweiler and Ernst (4). In their work they used a series of 180° pulses to accomplish the transfer of magnetization. The treatment presented by Braunschweiler and Ernst is based on isotropic mixing and

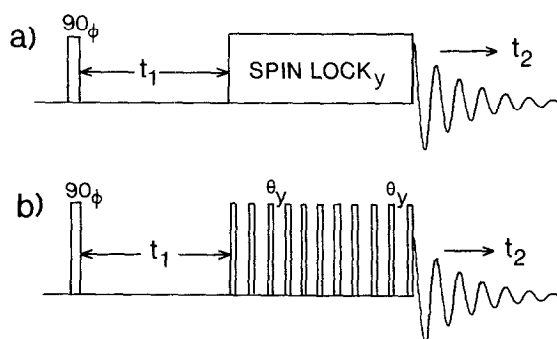


FIG. 1. Scheme of the 2D spin-locked NOE experiment (a) using a continuous spin-lock field and (b) using a pulsed spin-lock field, generated by the application of a series of pulses of small flip angle, θ ($\theta \ll \pi$) (9). The phase, ϕ , is cycled $x, y, -x, -y$ with the receiver phase $x, x, -x, -x$ and data for odd- and even-numbered scans are stored in separate locations. Alternatively, TPPI phase cycling of the first 90_ϕ pulse can be used.

their analysis does not predict the efficiency of magnetization transfer as a function of resonance offset. In the case where a continuous spin-lock field is used during the mixing period, as is the case in the spin-locked NOE experiment, the coherent magnetization transfer between spins can be considered a homonuclear analog of Hartmann–Hahn cross polarization (5, 6) and the off-resonance effects can be calculated directly, in a manner analogous to expressions derived by Müller and Ernst (7) and Chingas *et al.* (8). In this paper, first the magnetization transfer will be discussed for two protons, I and S, with scalar coupling J , using the regular spin-locked NOE experiment (1). Then, it will be shown that a modified version of the spin-locked NOE experiment that employs a series of equally spaced pulses of small flip angle (9) (Fig. 1b) results in identical amounts of coherent transfer as the regular spin-locked NOE experiment. Subsequently, a qualitative analysis will be presented of the effects of other spins coupled to I and S on the coherent transfer between I and S.

HOMONUCLEAR HARTMANN-HAHN CROSS POLARIZATION FOR TWO SPINS

The resonance offsets of two protons, I and S, are δ_I and δ_S , and the spin-lock field is of strength ν ; the effective fields are labeled ν_I and ν_S and make angles α_I and α_S with the positive z axis (Fig. 2). The difference, $\alpha_I - \alpha_S$, is labeled α . During the spin lock (along the y axis), the Hamiltonian is given by

$$\mathcal{H} = 2\pi\{\delta_I I'_z + \delta_S S'_z + \nu(I'_y + S'_y)\} + \mathbf{J}' \cdot \mathbf{S}' \}. \quad [1]$$

In this paper, all angular momentum operators with primes refer to the eigenbasis in the absence of the RF field; operators without primes refer to the basis where the RF field is present, with the z axis aligned along the effective field direction. It is convenient to compute the coherence transfer between I and S in the tilted frame of the magnetic fields (7), where the z axes are tilted to be parallel to their respective effective fields.

In this frame, the Hamiltonian is given by

$$\mathcal{H} = 2\pi[\nu_I I_z + \nu_S S_z + J\{I_x S_x + I_y S_y \cos \alpha + I_z S_z \cos \alpha + (I_z S_y - I_y S_z) \sin \alpha\}]. \quad [2]$$

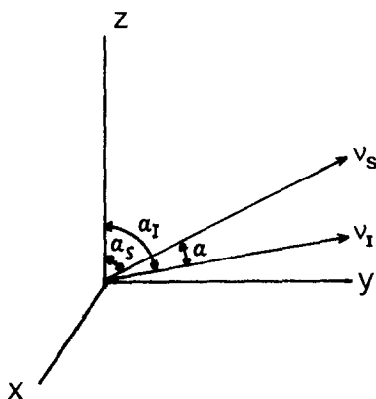


FIG. 2. Orientation of the effective spin-lock fields, ν_I and ν_S , in the rotating frame.

For sufficiently strong spin-lock fields, $\nu \gg J$, the nonsecular terms $I_z S_y$ and $I_y S_z$ may be neglected. The remaining scalar coupling part of the Hamiltonian may be rewritten as

$$\mathcal{H}_J = 2\pi J [I_z S_z \cos \alpha + (1 + \cos \alpha)(I^+ S^- + I^- S^+)/4 + (1 - \cos \alpha)(I^+ S^+ + I^- S^-)/4]. \quad [3]$$

Again, the $I^+ S^+$ and the $I^- S^-$ terms are nonsecular and may be neglected. As pointed out by Müller and Ernst, the remaining part of the Hamiltonian is very similar to the one for a strongly coupled spin system. Its four eigenvalues are

$$\begin{aligned} E_1 &= \{2(\nu_I + \nu_S) + J \cos \alpha\}/4 \\ E_2 &= -(J \cos \alpha)/4 + q \\ E_3 &= -(J \cos \alpha)/4 - q \\ E_4 &= \{-2(\nu_I + \nu_S) + J \cos \alpha\}/4 \end{aligned} \quad [4]$$

with

$$q = 1/2 \{(\nu_I - \nu_S)^2 + (1 + \cos \alpha)^2 J^2/4\}^{1/2}. \quad [5]$$

The stationary wavefunctions under spin-locked conditions are

$$\begin{aligned} \psi_1 &= |++\rangle \\ \psi_2 &= \cos \phi |+-\rangle + \sin \phi |--\rangle \\ \psi_3 &= -\sin \phi |+-\rangle + \cos \phi |--\rangle \\ \psi_4 &= |--\rangle \end{aligned} \quad [6]$$

with

$$\tan 2\phi = (1 + \cos \alpha)J/\{2(\nu_I - \nu_S)\}. \quad [7]$$

At the end of the evolution period, t_1 , the following magnetization components are present in the regular rotating frame: I'_x , I'_y , S'_x , S'_y , $I'_x S'_z$, $I'_y S'_z$, $S'_x I'_z$, and $S'_y I'_z$. The

presence of I'_z and S'_z at this point is removed by phase cycling of the first 90° pulse of the experiment. When the spin-lock field is applied along the y axis, the S'_x and I'_x terms are perpendicular to the effective RF fields and will rapidly defocus because of RF field inhomogeneity. To analyze the effect of the RF field on the remaining terms, these terms must be transformed into the tilted frame, as follows:

$$I'_y \xrightarrow{-\alpha_1 I'_x} \cos \alpha_1 I_y + \sin \alpha_1 I_z \quad [8]$$

$$I'_x S'_z \xrightarrow{-\alpha_1 I'_x - \alpha_S S'_x} \cos \alpha_S I_x S_z - \sin \alpha_S I_x S_y \quad [9]$$

$$I'_y S'_z \xrightarrow{-\alpha_1 I'_x - \alpha_S S'_x} \cos \alpha_1 \cos \alpha_S I_y S_z - \cos \alpha_1 \sin \alpha_S I_y S_y \\ + \sin \alpha_1 \cos \alpha_S I_z S_z - \sin \alpha_1 \sin \alpha_S I_z S_y \quad [10]$$

with analogous expressions for the remaining terms, S'_y , $S'_x I'_z$, and $S'_y I'_z$. Because of RF field inhomogeneity, in the tilted frame only z components and zero-quantum coherences survive for more than several milliseconds. Therefore the only terms of interest in this frame are I_z , S_z , $I_z S_z$, $I^+ S^-$, and $I^- S^+$. The product $I_z S_z$ commutes with the scalar coupling Hamiltonian and is a constant of motion. Any magnetization during the detection period originating from this term starts out in antiphase and does not make any net contribution to either diagonal or cross peaks. The terms $I^+ S^-$ and $I^- S^+$ are important and can be large. However, as is clear from Eqs. [9] and [10], they result from antiphase magnetization components in the regular rotating frame and therefore also do not contribute to the net magnetization transfer. The time dependence of I_z and S_z is straightforwardly calculated by transforming to the eigenbasis in which the Hamiltonian (Eq. [2]) is diagonal. Calculation of the evolution of the density matrix during spin lock and transforming back to the product basis gives

$$2I_z \xrightarrow{\mathcal{H}t} (1 + c^2 + s^2 \cos 2qt) I_z + s^2 (1 - \cos 2qt) S_z + R I^+ S^- + R^* I^- S^+ \quad [11]$$

with $c = \cos 2\phi$, $s = \sin 2\phi$, and $R = is(\sin 2qt) + cs(\cos 2qt - 1)$. The $I^+ S^-$ and $I^- S^+$ terms in Eq. [11] represent zero-quantum coherence in the tilted frame. After the spin-lock field is switched off these terms transfer into antiphase multiplet components along the $\pm x$ axis of the regular rotating frame. Therefore, these terms do not contribute to the integrated intensity of diagonal or cross peaks. As is also seen from Eq. [11], the net magnetization transferred from spin I to spin S equals $s^2(1 - \cos 2qt)$.

CONTINUOUS VS PULSED SPIN LOCK

In a recent report, Kessler *et al.* (9) proposed the use of a series of nonselective pulses of small flip angle θ ($\theta \ll \pi$) and of duration τ_p , spaced by short intervals, τ ($\tau \ll 1/\delta$), for spin locking the magnetization in the transverse NOE experiment (Fig. 1b). It is shown here that this is equivalent to a continuous spin lock with field strength $\theta/(\tau_p + \tau)$, and that this method does not increase suppression of J cross peaks over the original continuous spin-locked method.

During the pulse, the Hamiltonian is given by

$$\mathcal{H}_p = \nu I'_y + \mathcal{H}_{fp}, \quad [12]$$

where \mathcal{H}_{fp} is the free precession Hamiltonian:

$$\mathcal{H}_{fp} = \delta_I I'_z + \delta_S S'_z + J_{IS} \mathbf{I}' \cdot \mathbf{S}'. \quad [13]$$

Evolution of the density matrix, ρ , during a series of N pulses and delays is described by

$$\rho(N) = R^{-N} \rho(0) R^N, \quad [14]$$

with $R = \exp(i\mathcal{H}_p \tau_p) \exp(i\mathcal{H}_{fp} \tau)$. Using $\exp(iA) \exp(iB) = \exp\{i(A+B)\} \exp(i[A, B]/2)$, R can be rewritten as

$$R = \exp\{i(\mathcal{H}_p \tau_p + \mathcal{H}_{fp} \tau)\} \exp\{i\tau_p \tau [\mathcal{H}_p, \mathcal{H}_{fp}]\}. \quad [15]$$

Because $\mathcal{H}_p \tau_p \ll \pi$ and $\mathcal{H}_{fp} \tau \ll \pi$,

$$\exp\{i\tau_p \tau [\mathcal{H}_p, \mathcal{H}_{fp}]\} \approx 1 \quad [16]$$

yielding

$$R \approx \exp\{i(\mathcal{H}_p \tau_p + \mathcal{H}_{fp} \tau)\}. \quad [17]$$

Substitution in Eq. [14] shows that the pulsed spin-locked Hamiltonian is equivalent to the Hamiltonian, \mathcal{H} , given by

$$\mathcal{H} = \mathcal{H}_{fp} + \nu \tau_p / (\tau + \tau_p). \quad [18]$$

This proves that for resonance offsets much smaller than $1/\tau$, continuous spin locking with a field $\nu \tau_p / (\tau + \tau_p)$ is equivalent to applying a series of short pulses with RF field strength ν , duration τ_p , and spaced by intervals τ .

Figure 3 shows a comparison of the Fourier transform of the time dependence of $I'_y - S'_y$ during application of a continuous RF field of 4 kHz and during a series of 36° (5 μ s) pulses, using a 20 kHz RF field and pulse spacing of 20 μ s. In this simulation, spin I is on resonance and the offset of spin S is varied. The component at 0 Hz indicates I spin magnetization that is not transferred to spin S; the Fourier transform of the oscillatory transfer between I and S shows an increase in frequency of the transfer and a decrease in amplitude for increasing offsets of S, in agreement with Eq. [11]. As expected, comparison of Figs. 3a and 3b shows nearly identical behavior of the magnetization transfer as a function of S spin offset.

The RF power needed for generating a spin-lock field of identical effective strength is lower if continuous RF irradiation is used compared to pulsed irradiation. If, during the pulsed spin lock the duty cycle is $\tau_p / (\tau_p + \tau)$, the average power dissipated in the probe is $(\tau_p + \tau) / \tau_p$ higher than for a continuous spin-lock field of equivalent effective strength.

HARTMANN-HAHN CONTRIBUTIONS FOR MORE THAN TWO SPINS

All derivations presented above refer to the case of two scalar-coupled homonuclear spins in the absence of any other spins. Below, the effect of other spins on the I-S cross polarization will be analyzed in a qualitative manner. First, the case will be

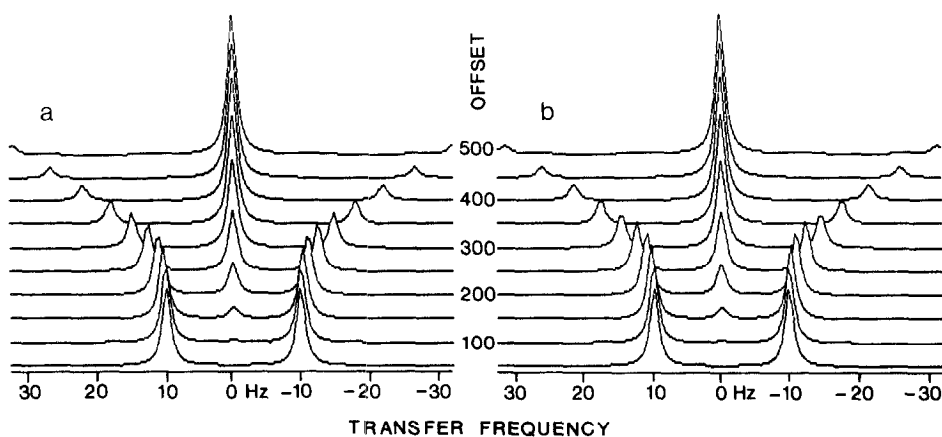


FIG. 3. Fourier transform of the time dependence of $I_y - S_y$ under two conditions: (a) a continuous 4 kHz spin-lock field applied along the y axis and (b) a pulsed spin-lock field consisting of 36° pulses ($5 \mu\text{s}$) separated by spacings of $20 \mu\text{s}$. In both cases, spin I is on resonance and the offset of spin S is varied from 50 to 500 Hz. At time 0, $I_y = 1$ and $S_y = -1$. The component at zero frequency corresponds to the fraction of the $I_y - S_y$ spin-locked magnetization that does not oscillate in amplitude. The exact computer simulation shows that for the small flip angles used (36°) the Hartmann-Hahn transfer is virtually identical to that obtained for a continuous spin-lock field with the same effective field strength. Spectra have been calculated with the program SPINCALC, kindly provided by Technic de Bouregas.

considered where only one extra spin, X, is present, assuming that the effective field for spin X, ν_X , differs significantly from ν_I and ν_S ; i.e.,

$$\begin{aligned} |\nu_X - \nu_I| &\gg |J_{IX}| \\ |\nu_X - \nu_S| &\gg |J_{SX}|. \end{aligned} \quad [19]$$

In this case the scalar coupling between I and X and between S and X is weak, and the scalar coupling part of the Hamiltonian under spin-locked conditions denoting the interaction between X and spins I and S simplifies to $J_{IX}I_zX_z\cos(\alpha_I - \alpha_X) + J_{SX}X_zS_z\cos(\alpha_S - \alpha_X)$. The part of the Hamiltonian during spin lock that describes interactions involving spins I and S (neglecting nonsecular terms) is given by

$$\begin{aligned} \mathcal{H}_{IS} = 2\pi[\nu_I I_z + \nu_S S_z + J_{IX}I_zX_z\cos(\alpha_I - \alpha_X) + J_{SX}S_zX_z\cos(\alpha_S - \alpha_X) \\ + J_{IS}\{(I_zS_z + I_yS_y)\cos(\alpha_I - \alpha_S) + I_xS_x\}]. \end{aligned} \quad [20]$$

This Hamiltonian has the same form as Eq. [2]; the only difference is that the effective field terms in Eq. [2], ν_I and ν_S , are modified by addition of $\pm\pi J_{IX}\cos(\alpha_I - \alpha_X)$ and $\pm\pi J_{SX}\cos(\alpha_S - \alpha_X)$, respectively. Therefore, analogous to the calculation of spectra of a conventional ABX spectrum (10), the magnetization transfer between I and S can be considered the sum of two transfers, with spin X parallel and antiparallel to the effective spin-lock field. The angle ϕ (Eq. [7]) must be redefined in this case as

$$\begin{aligned} \tan(2\phi^\pm) = \{1 + \cos(\alpha_I - \alpha_S)\}J_{IS}/[2(\nu_I - \nu_S) \\ \pm \{J_{IX}\cos(\alpha_I - \alpha_X) - J_{SX}\cos(\alpha_S - \alpha_X)\}], \end{aligned} \quad [21]$$

where ϕ^+ and ϕ^- refer to the ϕ value for spin X aligned parallel or antiparallel, respectively, to the X spin effective field. It is seen from this expression that the third spin, X, can modify the Hartmann–Hahn match condition for spins I and S. For example, if spins I and S experience the same effective RF field strengths (in the case where I and S are at equal but opposite offsets from the carrier) they are “mismatched” by the coupling to spin X by $\{J_{IX}\cos(\alpha_I - \alpha_X) - J_{SX}\cos(\alpha_S - \alpha_X)\}/2$. Similarly, if spins ν_I and ν_S are different, the X spin can improve the match condition for half of the I–S spin pairs (for example, for the systems where X is parallel to the effective field) and decrease the match condition for the other half of the I–S pairs. This is illustrated by the computer simulation in Fig. 4. Figure 4a shows the Fourier transform of the time dependence of $I_z - S_z$ during spin lock, in the absence of spin X, for a small mismatch of the effective RF fields ($\nu_I - \nu_S = 5$ Hz). As expected on the basis of Eq. [11], a fraction $\cos^2 2\phi$ ($\approx 20\%$) does not show any modulation, and a fraction $\sin^2 2\phi$ is modulated by $\cos 2qt$. By introducing a third spin, X, with $J_{IX} = 10$ Hz and $J_{SX} = 0$, the mismatch is removed for half of the spins but made worse for the other half of the spins (Fig. 4b). The unmodulated I spin component (at 0 Hz) is about 25% in Fig. 4b. For half of the IS pairs, the match condition is improved by coupling to spin X while worsened for the other half. The net effect is that the fraction of unmodulated spin-locked I spin magnetization remains nearly unchanged. It is also interesting to note that X causes the presence of two modulation frequencies instead of a single modulation frequency. If $|\nu_I - \nu_S| \gg |J_{IS}|, |J_{IX}|$, these two modulation frequencies become very similar (Eq. [21]).

It is clear from the above that the magnitude of the unmodulated fraction of I spin magnetization is affected only slightly by the presence of other spins, k , provided that

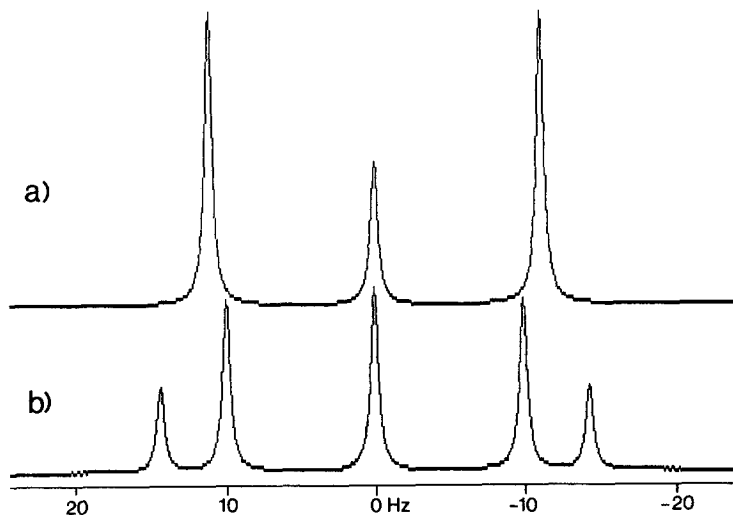


FIG. 4. Fourier transform of the time dependence of $I_z - S_z$ for two different spin systems: (a) an IS spin system and (b) an ISX spin system. The spin-lock field was 5 kHz, $J_{IS} = 10$ Hz, $J_{SX} = 10$ Hz, and $J_{IX} = 0$. The chemical shifts are $\delta_I = 0$, $\delta_S = 224$, and $\delta_X = 800$ Hz. Spectra are calculated with the SPINCALC program.

$$|\nu_I - \nu_S| > \sum_k |J_{ki} - J_{ks}|, \quad [22]$$

and

$$|\nu_I - \nu_k| \ll |J_{ki} - J_{ks}|; \quad |\nu_S - \nu_k| \ll |J_{ki} - J_{ks}|.$$

The transfer from I to S is still described, to a good approximation, by Eq. [11]. The presence of other spins causes a number of slightly different modulation frequencies that are usually not resolvable (in an experiment where the spin-lock period corresponds to the evolution period). Therefore, the oscillatory character of the modulation effect often disappears quite rapidly in practice. Moreover, because the modulation frequency depends on $\nu_I - \nu_S$, it is sensitive to RF inhomogeneity. Therefore the oscillatory character of the Hartmann–Hahn-type magnetization transfer is damped rapidly in practice. Figure 5 shows the oscillatory character of the spin-locked magnetization for one of the two C_β protons in c(D-Ala,L-Pro,L-Ala)₂ after the magnetizations of the two C_β protons are spin locked when they are in antiphase relative to one another in the transverse plane. The decay of spin-locked $C_\beta H(1)$ magnetization is shown for four different strengths of the spin-lock field. In all cases the oscillatory character of the spin-locked magnetization damps faster than the decay due to $T_{1\rho}$ relaxation. However, the weaker the spin-lock field, the larger the Hartmann–Hahn mismatch and the more rapid the damping of the oscillation becomes. The size of the modulated and unmodulated components is most easily measured by Fourier transforming the decays shown in Fig. 5, resulting in the spectra of Fig. 6. Integration of the resonance intensity at zero frequency relative to the total spectral intensity gives the fraction of unmodulated magnetization, which shows excellent agreement with values calculated using Eq. [11], assuming that the $C_\beta H$ protons form an isolated two-spin system.

Because the effective fields make angles α_I and α_S with the z axis, the fraction of transverse magnetization that will be spin locked is proportional to $\sin \alpha_I$ and $\sin \alpha_S$, for spin I and S, respectively. Only the fractions $\sin \alpha_I$ and $\sin \alpha_S$ of the spin-locked magnetizations are in the transverse plane after the spin-lock field is switched off. Neglecting Hartmann–Hahn effects, diagonal peaks of spins I and S are attenuated by factors $\sin^2 \alpha_I$ and $\sin^2 \alpha_S$, respectively. The (NOE/Hartmann–Hahn) cross peaks

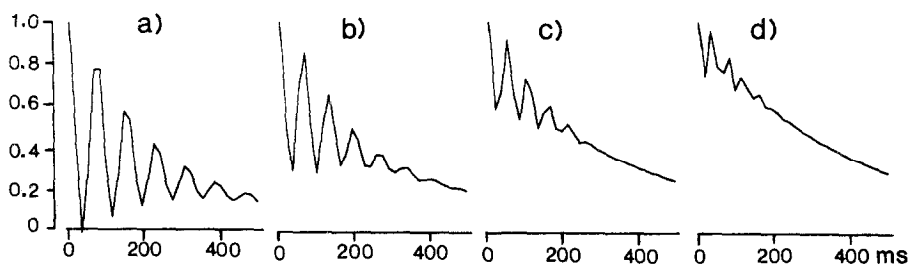


FIG. 5. Intensity of spin-locked magnetization of the downfield $C_\beta H$ proline resonance of c(D-Ala,L-Pro,L-Ala)₂ as a function of spin-lock time for four different strengths of the spin-lock field: (a) 9.1 kHz, (b) 6.7 kHz, (c) 4.6 kHz, and (d) 3.3 kHz. The carrier was placed 380 Hz downfield of the observed proton resonance. The second $C_\beta H$ proton resonates at 570 Hz offset. The spin lock was started when the magnetizations of the two $C_\beta H$ protons were aligned in antiphase along the $\pm y$ axis by inserting a delay of 2.63 ms after the initial 90°_x excitation pulse. The geminal coupling between the two $C_\beta H$ protons is 10.0 Hz.

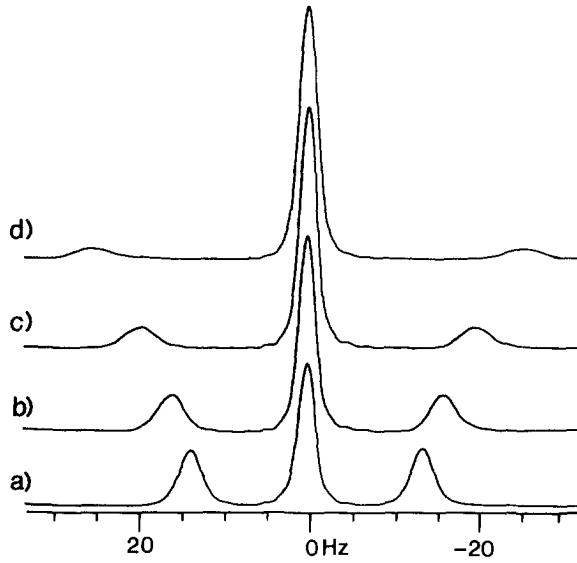


FIG. 6. Fourier transforms of the time-domain data of Fig. 5. The unmodulated component measured from these spectra represents (a–d) 45, 64, 79, and 85.5%. Calculated values are 49, 65, 81, and 88%, respectively.

are attenuated by factors $\sin \alpha_I \sin \alpha_S$. The diagonal peaks are further attenuated by factors $s^2(1 - \cos 2qt)$ and the cross peaks have a Hartmann–Hahn contribution which is in-phase with the diagonal resonances proportional to $s^2(1 - \cos 2qt)$. Apart from NOE and relaxation effects, the relative intensities in the spin-locked NOE spectrum are therefore given by

$$\begin{aligned} II &= 1/2 \sin^2 \alpha_I (1 + c^2 + s^2 \cos 2qt) \\ IS = SI &= 1/2 \sin \alpha_I \sin \alpha_S s^2 (1 - \cos 2qt) \\ SS &= 1/2 \sin^2 \alpha_S (1 + c^2 + s^2 \cos 2qt). \end{aligned} \quad [23]$$

Superimposed on these intensities are the effects of the spin-locked NOE of interest. The spin-locked cross-relaxation rate between spins I and S, σ_{IS} , is modified under off-resonance conditions by (11, 12)

$$\sigma_{IS} = \sin \alpha_I \sin \alpha_S \sigma_{IS_{tr}} + \cos \alpha_I \cos \alpha_S \sigma_{IS_{ln}}, \quad [24]$$

where $\sigma_{IS_{tr}}$ and $\sigma_{IS_{ln}}$ are the transverse (I) and longitudinal cross-relaxation rates. For most cases of interest $\sigma_{IS_{ln}}$ will be significantly smaller than $\sigma_{IS_{tr}}$, so the longitudinal contribution (with the small coefficient $\cos \alpha_I \cos \alpha_S$) usually may be neglected.

I–S NOE in the presence of I–S coupling. When measuring the spin-locked NOE between coupled spins, the cross-peak intensities must be corrected for Hartmann–Hahn contributions. As discussed above, under mismatched conditions the amount of Hartmann–Hahn transfer has a quadratic dependence on the size of the J coupling. Since the size of this coupling may not be known accurately, and because there also is a weak dependence on the presence of other spins coupled to I or S, a reliable

measurement of the NOE component becomes very difficult for systems where the Hartmann–Hahn component is stronger than the NOE component. If the Hartmann–Hahn contribution is of similar magnitude or smaller than the NOE contribution, two cases must be considered separately. First, if the difference in effective field strengths is much larger than the reciprocal of the mixing time

$$|\nu_1 - \nu_S| \gg \tau_m^{-1} \quad [25]$$

the oscillatory I–S transfer (Eq. [11]) will have damped out by the end of the mixing period, and Eq. [23] simplifies to

$$\begin{aligned} II &= 1/2 \sin^2 \alpha_I (1 + c^2) \\ IS = SI &= 1/2 \sin \alpha_I \sin \alpha_S s^2 \\ SS &= 1/2 \sin^2 \alpha_S (1 + c^2). \end{aligned} \quad [26]$$

For short mixing times, where condition [25] is not satisfied, the Hartmann–Hahn contribution can be averaged by adding a small random variation to the length of the mixing period, analogous to the random variation used in NOESY experiments for eliminating zero-quantum contributions (13). For expression [26] to become applicable, the random part of the spin-lock period should be at least of length $1/|\nu_1 - \nu_S|$. Of course, if the NOE contribution to a cross peak is much larger than s^2 , such random variation of the mixing time will not be necessary unless a very accurate measurement of the NOE is required.

K–I NOE in the presence of I–S coupling. In practice, two spins K and I that have an NOE interaction will often be scalar coupled to other spins. This not only affects the KI NOE intensity but also can give spurious KS NOE cross peaks if spins I and S are scalar coupled (2, 14). As before, a simple reliable estimate of the Hartmann–Hahn effects requires that there is a significant mismatch ($\phi < 15^\circ$) and that the transfer frequencies (2q) are greater than $1/\tau_m$. In the absence of I–S coupling, the transfer of magnetization from K to I via the NOE effect can be described by a function, $f(t)$. To a first approximation, the relay from K to S is then given by

$$KS = 0.5 \sin \alpha_K \sin \alpha_S \int_0^{\tau_m} f(t) s^2 \{1 - \cos 2q(\tau_m - t)\} dt. \quad [27]$$

Since $f(t)$ is a slowly growing function ($f(1/2q) \ll 1$) and $\tau_m \gg 1/2q$, the KS transfer can be approximated by

$$KS = 0.5 \sin \alpha_K \sin \alpha_S f(\tau_m) s^2. \quad [28]$$

Similarly, because of the I–S relay the KI NOE cross-peak intensity will change by a factor, β , given by

$$\beta = 1 - 0.5s^2. \quad [29]$$

For interactions involving equivalent methylene protons or methyl groups, the rate of Hartmann–Hahn transfer under strongly mismatched conditions ($|J| \ll |\nu_{\text{Ieff}} - \nu_{\text{Seff}}|$) remains unchanged to first order relative to the IS case. However, the amplitudes of the oscillation increase by factors of 2 and 2.5 for IS₂ and IS₃ systems, respectively (7). The semiquantitative analysis presented above is valid only if there are no other nuclei present that have a good Hartmann–Hahn match ($\phi > 15^\circ$) with spin S.

A TYPICAL EXAMPLE

All correction factors derived above apply to the integrated multiplet intensities. Homonuclear Hartmann–Hahn transfer causes both net transfer and antiphase transfer. The antiphase component does not change the integrated peak intensity but generally will affect the maximum peak intensity. Averaging over a number of slightly different mixing times (see above) can eliminate the antiphase components (4).

In practice, the correction factors are quite small for the majority of connectivities in peptides. This is demonstrated by examining a typical example, the interactions involving the NH resonance of Tyr-21 in BPTI. A 2D spin-locked NOE spectrum has been recorded in H₂O at 500 MHz, with the carrier positioned on the H₂O resonance at 4.65 ppm and a 6.3 kHz spin-lock RF field. Further details about the particular pulse scheme used in H₂O are presented elsewhere (15).

Direct Hartmann–Hahn contributions. The F_1 trace through the 2D spin-locked NOE spectrum taken at the F_2 frequency of the Tyr-21-NH proton is shown in Fig. 7a. For comparison, the corresponding F_1 trace taken through a NOESY spectrum with 120 ms mixing time is shown in Fig. 7b. The NH, C_αH, and C_βH₂ shifts are 9.2, 5.7, and 2.75 ppm, respectively. The effective RF fields make angles of $\alpha_N = 70.2^\circ$, $\alpha_\alpha = 85.2^\circ$, and $\alpha_\beta = 98.8^\circ$ with the positive z axis for the NH, C_αH, and C_βH₂ protons, respectively. The strength of the effective spin-lock fields for the three resonances are 6.698, 6.322, and 6.371 kHz. The couplings in Tyr-21 are $J_{\text{NH-C}\alpha\text{H}} = 10$ and $J_{\text{C}\alpha\text{H-C}\beta\text{H}_2} = 6.5$ Hz. Besides NOE effects, the relative intensities of the NH diagonal resonance and the NH–C_αH Hartmann–Hahn cross peak follow from Eq. [26]. Their

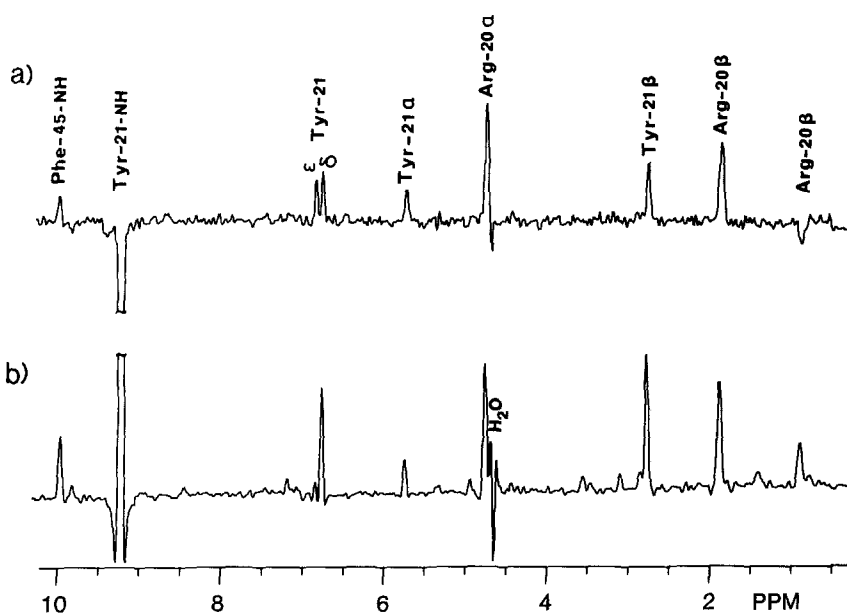


FIG. 7. Cross sections through the (a) ROESY and (b) NOESY spectra of BPTI, taken parallel to the F_1 axis at the F_2 frequency of the Tyr-21-NH resonance. Both spectra were recorded at 500 MHz using nearly identical total measuring times (16 h). Temperatures were slightly different: 37°C (ROESY) and 42°C (NOESY), and the mixing times were 60 ms (ROESY) and 120 ms (NOESY).

intensities are 0.88 and 6.6×10^{-4} , respectively. This shows that the Hartmann–Hahn contribution to the NH–C $_{\alpha}$ H cross peak is extremely small (<0.1%) relative to the diagonal peak intensity. Note however, that a similar analysis for the C $_{\alpha}$ H–C $_{\beta}$ H₂ Hartmann–Hahn contribution yields a 1.7% cross peak which could constitute a significant fraction of the C $_{\alpha}$ H–C $_{\beta}$ H₂ NOE cross-peak intensity.

Relay of NOE via Hartmann–Hahn. Using Eq. [28] with the assumption that the C $_{\beta}$ H₂ protons are equivalent, the amount of relay of the C $_{\alpha}$ H–NH NOE cross peak to the C $_{\beta}$ H₂ protons is 1.7%. This demonstrates that only a very small fraction of the NH–C $_{\alpha}$ H NOE cross-peak intensity is relayed to the C $_{\beta}$ H₂ protons. A much stronger relay is observed for the aromatic ring protons. The regular NOE spectrum (Fig. 7b) shows NOE connectivity to the C $_{\delta}$ H protons only, whereas the spin-locked NOE spectrum displays nearly equal intensity cross peaks to the C $_{\delta}$ H (6.73 ppm) and C $_{\epsilon}$ H (6.81 ppm) protons. Since the mismatch of the C $_{\delta}$ H and C $_{\epsilon}$ H protons is now quite small ($\phi = 25^\circ$), expressions [28] and [29] are no longer strictly valid and relay from C $_{\delta}$ H to C $_{\epsilon}$ H is nearly complete. The Tyr-21-NH proton also shows an intense NOE connectivity to a C $_{\beta}$ H proton of Arg-20 at 1.86 ppm. In principle, one might expect Hartmann–Hahn relay to the second C $_{\beta}$ H proton at 0.87 ppm. However, the mismatch for these two methylene protons is large ($\phi = 2.7^\circ$, based on a 12 Hz geminal coupling), relaying only 0.5% relay intensity (Eq. [28]) to the second C $_{\beta}$ H proton. Figure 7a shows a cross peak to the second C $_{\beta}$ H proton that is opposite to the regular NOE cross peaks, indicating that this relay is caused by the (three-spin) NOE effect (2), which apparently is much larger than the Hartmann–Hahn relay contribution. Note that for the 120 ms mixing time NOESY spectrum (Fig. 7b) the NOE cross peaks to the two C $_{\beta}$ H protons are of comparable magnitude, while the cross peak to the proton at 0.87 ppm is almost entirely caused by spin diffusion.

Offset effects. As pointed out previously (3), Hartmann–Hahn effects can be minimized by a suitable choice of the RF carrier position and by using a relatively weak spin-lock RF field. The necessity of using a relatively weak RF field leads to substantial intensity distortions near the edges of the spectrum. Consider, for example, the Tyr-21-NH/Phe-45-NH cross peak in Fig. 7a. The two protons resonate at 9.2 and 10.0 ppm, respectively, corresponding to off-resonance angles (α_1 and α_2) of 70° and 67° . According to Eq. [24], the transverse component of the cross relaxation is decreased by $\sin(70^\circ)\sin(67^\circ) \approx 0.86$. For macromolecules, the longitudinal component of the cross relaxation is opposite in sign and approximately half the size relative to the transverse cross relaxation, giving a contribution of $-0.5\cos(67^\circ)\cos(70^\circ) = -0.07$. Therefore the apparent NOE buildup rate will be scaled down by a factor $0.86 - 0.07 = 0.79$. The cross-peak intensity is further scaled down by a factor $\sin(67^\circ)\sin(70^\circ)$ because of off-resonance effects (Eq. [23]), resulting in total cross-peak attenuation by a factor of 0.68.

DISCUSSION

This paper presents guidelines for estimating semiquantitatively the intensity distortions originating from nonnegligible RF offset effects and from homonuclear Hartmann–Hahn transfers in a spin-locked NOE experiment. In practice, measurement of an NOE intensity with $\pm 10\%$ accuracy is often sufficient and therefore for most

NOE cross peaks it will not be necessary to calculate correction factors. However, as discussed above, Hartmann–Hahn effects can become very important when measuring NOEs between scalar-coupled protons that experience a similar absolute magnitude of the effective RF field. In particular, measurement of NOEs between protons that are close in chemical shifts may be seriously affected. For these resonances a semi-quantitative analysis of the possible Hartmann–Hahn effects will be necessary before a quantitative interpretation of the resonance intensities can be made. Also, if an NOE is observed to two or more protons that are scalar coupled, one should analyze whether these cross peaks could be caused by a single NOE interaction combined with Hartmann–Hahn relay.

The presence of Hartmann–Hahn magnetization transfer in ROESY spectra presents considerably more difficulty than the presence of analogous zero-quantum coherence transfer in NOESY spectra. Compounds, such as sugars, alkaloids, and steroids, that typically have a large number of scalar-coupled protons within a relatively narrow bandwidth may not be very suitable for study with the ROESY experiment. A large number of the possible interproton distances in these molecules may be difficult or impossible to measure with the ROESY method. It appears to be fundamentally impossible to develop a method that measures the transverse NOE without the introduction of Hartmann–Hahn artifacts. In principle, the best approach for minimizing these artifacts is to use a very strong RF field of N kHz, with the carrier positioned at a distance of about $N/3$ kHz away from the center of the spectrum. In practice, this is inconvenient because it requires a spectral window in the F_2 dimension much larger than the spectral width and the strong RF field would create RF heating problems during the mixing period. A better choice therefore is to use a relatively weak RF field, judiciously positioned such that Hartmann–Hahn matching effects are minimized (3, 16).

Under well-adjusted conditions, the ROESY technique can yield spectra of quality comparable to NOESY spectra for macromolecules. The main advantage of the ROESY method is for molecules that have a near-zero regular NOE, whereas the spin-locked NOE can be as large as 0.5. Other advantages of ROESY are that chemical exchange peaks are easily recognized (1, 17) and that spin diffusion effects tend to be small and identifiable. The guidelines presented in this paper permit making an estimate of the size of the Hartmann–Hahn contribution to NOE cross peaks. These guidelines may be used for more reliable measurements of the spin-locked NOE buildup rates, which may result in more accurate determinations of three-dimensional structures.

ACKNOWLEDGMENTS

I thank Rolf Tschudin for continuous technical support, Donald Davis for a preprint of Ref. (11), Laura Lerner for suggestions during the preparation of the manuscript, and Attila Szabo for helpful discussions. The SPINCALC program was kindly provided by J. S. Waugh.

Note added in proof: In a recent paper, Griesinger and Ernst (*J. Magn. Reson.* 75, 261) describe an elegant modification of the ROESY experiment that eliminates the projection terms $\sin^2\alpha_1$, $\sin\alpha_1\sin\alpha_S$ and $\sin^2\alpha_S$ from Eqs. [23], [24], and [26]. Moreover, they discuss in detail the multiplet effects induced by the I_xS_z terms of Eq. [10].

REFERENCES

1. A. A. BOTHNER-BY, R. L. STEPHENS, J. T. LEE, C. D. WARREN, AND R. W. JEANLOZ, *J. Am. Chem. Soc.* **106**, 811 (1984).
2. A. BAX, V. SKLENÁŘ, AND M. F. SUMMERS, *J. Magn. Reson.* **70**, 327 (1986).
3. A. BAX AND D. G. DAVIS, *J. Magn. Reson.* **63**, 207 (1985).
4. L. BRAUNSCHEILER AND R. R. ERNST, *J. Magn. Reson.* **53**, 521 (1983).
5. S. R. HARTMANN AND E. L. HAHN, *Phys. Rev.* **128**, 2042 (1962).
6. A. PINES, M. G. GIBBY, AND J. S. WAUGH, *J. Chem. Phys.* **59**, 569 (1973).
7. L. MÜLLER AND R. R. ERNST, *Mol. Phys.* **38**, 963 (1979).
8. G. C. CHINGAS, A. N. GARROWAY, R. D. BERTRAND, AND W. B. MONIZ, *J. Chem. Phys.* **74**, 127 (1981).
9. H. KESSLER, C. GRIESINGER, R. KERSSEBAUM, K. WAGNER, AND R. R. ERNST, *J. Am. Chem. Soc.* **109**, 607 (1987).
10. J. A. POPLE, W. G. SCHNEIDER, AND H. J. BERNSTEIN, "High Resolution Nuclear Magnetic Resonance," p. 132, McGraw-Hill, New York, 1959.
11. D. G. DAVIS, *J. Am. Chem. Soc.* **109**, 3471 (1987).
12. B. T. FARMER AND L. R. BROWN, *J. Magn. Reson.* **72**, 197 (1987).
13. M. RANCE, G. BODENHAUSEN, G. WAGNER, K. WÜTHRICH, AND R. R. ERNST, *J. Magn. Reson.* **62**, 497 (1985).
14. D. NEUHAUS AND J. KEELER, *J. Magn. Reson.* **68**, 568 (1986).
15. A. BAX, V. SKLENÁŘ, G. M. CLORE, AND A. GRONENBORN, *J. Am. Chem. Soc.* **109**, 6511 (1987).
16. M. F. SUMMERS, L. G. MARZILLI, AND A. BAX, *J. Am. Chem. Soc.* **108**, 4285 (1986).
17. D. G. DAVIS AND A. BAX, *J. Magn. Reson.* **64**, 533 (1985).